

**NASA TECHNICAL  
REPORT**



**NASA TR R-365**

*a. 1*

**NASA TR R-365**

**LOAN COPY: RETURN  
AFWL (DOGL)  
KIRTLAND AFB, N. M.**

0068447



**TECH LIBRARY KAFB, NM**

**ANALYSIS OF SEVERAL RELATIONS  
AMONG ATMOSPHERIC STATISTICS**

*by R. A. Minzner and P. Morgenstern*

*Electronics Research Center*

*Cambridge, Mass. 02139*





0068447

1. Report No. NASA TR R-365		2. Government Accession No.		3. Recipient's Catalog No.	
4. Title and Subtitle ANALYSIS OF SEVERAL RELATIONS AMONG ATMOSPHERIC STATISTICS				5. Report Date March 1971	
				6. Performing Organization Code	
7. Author(s) R.A. Minzner and P. Morgenstern				8. Performing Organization Report No. C-113	
9. Performing Organization Name and Address  Electronics Research Center Cambridge, Mass.				10. Work Unit No. 125-06-03	
				11. Contract or Grant No.	
12. Sponsoring Agency Name and Address  National Aeronautics and Space Administration Washington, D. C. 20546				13. Type of Report and Period Covered  Technical Report	
				14. Sponsoring Agency Code	
15. Supplementary Notes					
16. Abstract A statistical equation relating the mean values of pressure, temperature, and density in a gas-law-like expression includes (in addition to the regular gas-law-like terms) a correction term proportional to the covariance between density and temperature. The application of the data from a set of 437 rocket soundings showed the value of the covariance term to be generally in the range $\pm 1.0$ percent of the mean pressure for altitudes of 30 to 60 km. The covariance was largest at the greater altitudes, in arctic latitudes, and during winter months. The application of the same data sets to another statistical equation relating $\partial\sigma\{p\}/\partial z$ (the derivative of the standard deviation of pressure with respect to altitude) to $\sigma\{p\}$ (the standard deviation of density) in a form suggestive of the hydrostatic equation (which relates $\partial p/\partial z$ to $\rho$ ) yielded very poor agreement, undoubtedly owing to large uncertainties in the observed values of $\partial\sigma\{p\}/\partial z$ . An integral form of the same equation, however, served to predict the observed data rather well.					
17. Key Words .Aeronomy .Atmospheric thermodynamics .Upper atmosphere soundings .Atmospheric statistics				18. Distribution Statement  Unclassified - Unlimited	
19. Security Classif. (of this report)  Unclassified		20. Security Classif. (of this page)  Unclassified		21. No. of Pages 39	
				22. Price* \$3.00	

# ANALYSIS OF SEVERAL RELATIONS AMONG ATMOSPHERIC STATISTICS

By R. A. Minzner\* and P. Morgenstern†

## SUMMARY

A statistically rigorous equation relating  $\bar{p}$ ,  $\bar{T}$ , and  $\bar{\rho}$ , the mean values of pressure, temperature, and density, respectively, into a gas-law-like expression includes (in addition to the regular gas-law-like terms) a correction term proportional to the covariance between density and temperature. The application of the data from a set of 437 rocket soundings and several quasi-homogeneous subsets of the same data showed the value of the covariance term to be generally in the range of +1 to -1 percent of  $\bar{p}$  for altitudes of 30 to 60 km. Covariance term values increased at greater altitudes and were largest for arctic latitudes and winter months. The application of the same data sets to another statistical equation relating  $\partial\sigma\{p\}/\partial z$  (the derivative of the standard deviation of pressure with respect to altitude) to  $\sigma\{\rho\}$  (the standard deviation of density) in a form suggestive of the hydrostatic equation (which relates  $\partial p/\partial z$  to  $\rho$ ) yielded very poor agreement, undoubtedly owing to large uncertainties in the observed values of  $\partial\sigma\{p\}/\partial z$ . An integral form of the same equation, however, served to predict the observed data rather well.

## I. INTRODUCTION

It has been customary in the generation of model atmospheres during the past decade (refs. 1-7) to use the following procedure:

1. Determine a mean altitude profile for a single thermodynamic atmospheric variable from available sounding data,
2. Introduce this altitude profile into the hypsometric equation and the gas law (or equation of state), and compute the model altitude profiles of other thermodynamic properties.

Thus, while the model atmosphere appears to be generally consistent with the mean values of temperature, pressure, and density deduced from sounding data, the model was derived as if there had been but a single sounding. It may be demonstrated that the mean value of density and the mean value of pressure

---

\*Electronics Research Center, Cambridge, Mass.

†Walden Research Corporation, Cambridge, Mass.

at a particular altitude calculated directly from the basic data of a number of soundings would not necessarily agree with the corresponding values of density and pressure as deduced by the above model-generation procedure. The implication of this situation is that while the simple form of the gas law quite accurately relates the thermodynamic properties of the atmosphere for a single sounding, it does not in general rigorously relate the corresponding mean values derived from a number of soundings.

The gas law (or equation of state for an ideal gas) relating pressure,  $p$ , temperature,  $T$ , and density,  $\rho$ , can be expressed as

$$p = \frac{R}{M} \rho \cdot T \quad (1)$$

where  $M$  is the mean molecular weight of air and  $R$  is the universal gas constant. The point values for  $p$ ,  $\rho$ , or  $T$  may be expressed as the sum of the corresponding mean values,  $\bar{p}$ ,  $\bar{\rho}$ , or  $\bar{T}$ , and of the departures,  $p'$ ,  $\rho'$ , or  $T'$ , respectively, as follows:

$$p = \bar{p} + p' \quad (2)$$

$$\rho = \bar{\rho} + \rho' \quad (3)$$

$$T = \bar{T} + T' \quad (4)$$

Substituting Eqs. (2), (3), and (4) into Eq. (1), and performing the indicated multiplications produces a second form of the gas law which, like Eq. (1), is also applicable only to a single set of conditions, i.e., only to a single sounding at a given altitude.

$$\bar{p} + p' = \frac{R}{M} [\bar{\rho} \cdot \bar{T} + \bar{\rho} \cdot T' + \rho' \cdot \bar{T} + \rho' \cdot T'] \quad (5)$$

Applying the averaging operator to both sides of Eq. (5) and noting that

$$\overline{T'} = \overline{p'} = \overline{\rho'} = 0$$

yields the result

$$\bar{p} = \frac{R}{M} [\bar{\rho} \cdot \bar{T} + \overline{\rho' \cdot T'}] \quad (6)$$

where the quantity  $\overline{\rho'T'}$  is commonly termed the covariance between  $\rho$  and  $T$ . Thus, the procedure for developing model atmospheres described above is strictly valid only if the covariance is equal to zero.

Equation (6) can also be expressed in the alternate form

$$\bar{p} = \frac{R}{M} [\bar{\rho} \cdot \bar{T} + \sigma\{\rho\} \cdot \sigma\{T\} \cdot r\{\rho, T\}] \quad (7)$$

where  $\sigma\{\rho\}$  and  $\sigma\{T\}$  are the standard deviation of density and temperature, respectively, and  $r\{\rho, T\}$  is the coefficient of correlation between them. Since  $\sigma\{\rho\}$  and  $\sigma\{T\}$  are almost always non-zero, this equation shows that the stated procedure for developing model atmospheres is strictly valid only if the correlation between  $\rho$  and  $T$  is zero. Both, Eqs. (6) and (7), are statistical forms of the gas law as derived by Buehl (ref. 8).

The covariance term in Eq. (6) represents the correction necessary to make the gas law strictly valid when applied to mean values for the thermodynamic properties. Stated another way, the covariance term is a measure of the error incurred during the development of model atmospheres by the method described earlier. Normalizing this error relative to the total pressure and converting the ratio to a percentage, the error may be expressed as

$$\text{percentage contribution of covariance term} = 100 \frac{R}{M} \cdot \frac{\overline{\rho'T'}}{\bar{p}} \quad (8)$$

Further insight into the factors contributing to this error term may be obtained by rearranging terms in Eq. (7) to produce

$$\bar{p} = \frac{R}{M} \bar{\rho} \cdot \bar{T} \left[ 1 + \frac{\sigma\{\rho\}}{\bar{\rho}} \cdot \frac{\sigma\{T\}}{\bar{T}} \cdot r\{\rho, T\} \right] \quad (9)$$

Thus the error term is the product of the coefficient of correlation between density and temperature, and of the coefficients of variation\* of these two properties. The sign of the correction term is determined by the sign of the correlation coefficient since the other two quantities are always positive.

---

\*The coefficient of variation is defined as the ratio of the standard deviation to the mean value.

Another model relating statistical properties of atmospheric thermodynamic variables uses the hydrostatic equation as its primary basis. The standard form of the hydrostatic equation is

$$\frac{\partial p}{\partial z} = -g \cdot \rho \quad (10)$$

where  $g$  is the acceleration of gravity and  $z$  is geometric altitude. It follows from Eqs. (2) and (3) that the hydrostatic equation also may be expressed as:

$$\frac{\partial p'}{\partial z} = -g \cdot \rho' \quad (11)$$

From the basic statistical definition of the standard deviation, we have

$$[\sigma\{p\}]^2 = \overline{p' \cdot p'} \quad (12)$$

Differentiating both sides of this equation with respect to  $z$  produces

$$\sigma\{p\} \frac{\partial \sigma\{p\}}{\partial z} = \overline{p' \frac{\partial p'}{\partial z}} \quad (13)$$

Substituting Eq. (11) into the right side of (13) yields

$$\sigma\{p\} \frac{\partial \sigma\{p\}}{\partial z} = -g \cdot \overline{p' \cdot \rho'} \quad (14)$$

where  $g$  may be considered constant for a given latitude and given height\*. By means of the definition of the correlation coefficient, this equation can be expressed finally in the form

$$\frac{\partial \sigma\{p\}}{\partial z} = -g \cdot \sigma\{\rho\} \cdot r\{\rho, p\} \quad (15)$$

where  $\sigma\{\rho\}$  is the standard deviation of density as before, and  $r\{p, \rho\}$  is the correlation coefficient between pressure and density.

---

\*These restrictions could be removed by using geopotential,  $H$ , rather than the geometric height,  $z$ . This was not done in the present study.

This is the expression derived by Buell (ref. 9) for the vertical gradient of the standard deviation of pressure at a constant height. It is analogous to an expression derived by Stidd (ref. 10) for the vertical gradient of the standard deviation of height on a constant pressure surface.

The validity of Eqs. (6) and (15) was examined for the 30 to 200 km region of the atmosphere by Minzner and Morgenstern (ref. 11). The data collected for this purpose consisted of 437 upper-air soundings covering the period 1947 to early 1965. These basic data were collected from 48 different sources including journal articles, institutional reports, and private communications. The data sample includes a variety of measurement techniques (falling-sphere, search-light probe, rocket-grenade, pitot-static probe, etc.), and covers a world-wide distribution of 25 launch sites. The data set is considered to be a unique collection of upper-air soundings; it has been published in a separate technical report by Minzner, Morgenstern, and Mello (ref. 12).

The 437 soundings were stratified into quasi-homogeneous groups by a diurnal, seasonal, and latitudinal classification scheme. The samples within each of these subsets were used to validate the two statistical models, and disclose any observed time and/or space variations in the results.

The model for the gas law was tested by evaluating the percentage contribution of the covariance-correction term to the total mean pressure (see Eq. (8)). This quantity was calculated at integral kilometer altitudes for each of the diurnal-seasonal-latitudinal subsets of the data. The results were presented as an extensive set of 110 machine-plotted graphs (ref. 11).

The model based on the hydrostatic equation was tested by evaluating the expression:

$$\text{percentage difference} = 100 \frac{\frac{\partial \sigma\{p\}}{\partial z} - [-g \cdot \sigma\{\rho\} \cdot r\{p, \rho\}]}{\frac{\partial \sigma\{p\}}{\partial z}} \quad (16)$$

The statistical quantities  $\sigma\{p\}$ ,  $\sigma\{\rho\}$ , and  $r\{p, \rho\}$  were calculated at integral kilometer altitudes for each of the diurnal-seasonal-latitudinal data subsets. The value of  $\partial \sigma\{p\} / \partial z$  was calculated using Stirling's central-difference formula (ref. 13) for numerical differentiation:

$$\frac{\partial \sigma\{p\}}{\partial z} \sim \frac{1}{\Delta z} \left[ \frac{f\{z_1\} - f\{z_{-1}\}}{2} - \frac{f\{z_2\} - 2f\{z_1\} + 2f\{z_{-1}\} - f\{z_{-2}\}}{12} + \dots \right] \quad (17)$$

where  $\Delta z$  is the altitude increment between successive points (in this case 1 km), and  $f\{z_i\}$  is the value of  $\sigma\{p\}$  at  $i$  altitude increments removed from the central value. A minimum of three points (one point on either side of the central value) and a maximum of five points (two points on either side of the central value) were used to evaluate the derivative. The results of the evaluation of Eq. (16) also have been presented as a set of 110 machine-plotted graphs (ref. 11).

## II. DISCUSSION OF RESULTS FROM THE GAS LAW MODEL

### Variability of the Covariance Term in the Gas Law Model

The graphs presented by Minzner and Morgenstern (ref. 11) are accompanied by a preliminary discussion of the physical implications. A more comprehensive review of the calculations and graphical results described previously has been conducted subsequent to the original publication. The results of this analysis are summarized below in terms of observed significant time and space variations.

#### 1. Height Variations

- a. Between 30 and 60 km, the magnitude of the correction term is usually much less than 1 percent, and only rarely exceeds 0.1 percent (to about 0.5 percent).
- b. The magnitude of the correction term tends to be greater for altitudes between 60 and 115 km than for altitudes below 60 km, but its value is still usually small compared with 1 percent for most of the stratified data sets. The number of data cells for which the values of the correction term exceed 1 percent for short altitude intervals increases with decreasing sample size at the higher altitudes. To increase the sample size at these altitudes, the data in different latitude belts were combined into a single subset. Combining these data introduces greater heterogeneity into the sample, resulting in increased correction-term values which grow to as much as 2 or 3 percent especially above 90 km. (Only for those data cells which present grouping of subsets across latitude bands is the sample size as large as 9 or more above 90 km.\*)
- c. All the data were grouped into a single data set to provide a sample size of 9 or more extending above 115 km.

---

\*A minimum sample size of 9 soundings was considered necessary to provide significant results.



In this case the value of the correction term increased to 5 percent between 115 and 155 km, whereas above this region its value increased to as much as 25 percent at 210 km.

## 2. Latitudinal Variations

- a. For the altitude region 30 to 60 km, the value of the correction term tends to increase with increasing latitude. For the basic homogeneous data cells, this increase varies from  $\leq 0.1$  percent in the tropics to  $\leq 0.5$  percent in the arctic.
- b. For data cells combined across seasons and diurnal periods, the increased heterogeneity resulting from these compressions causes the value of the correction term to increase from 0.1 percent or less in the altitude region of 30 to 60 km in the tropics to values as great as 2 percent for the same altitude region in the arctic.
- c. In the altitude region of 60 to 100 km, the trend is not so distinct since the number of available data sets is considerably less. The variation seems to be from values  $< 0.7$  percent in the tropics to  $\leq 3.8$  percent in the mid-latitude and subarctic belts. No arctic values are available at these altitudes.

## 3. Seasonal Variations

- a. In the high latitudes, a strong seasonal variability is seen whereby the value of the correction term tends to increase from  $\leq 0.1$  percent in summer to  $< 1.4$  percent in winter, in the altitude region of 30 to 80 km.
- b. No significant trend in the variability of the value of the correction term as a function of season has been noted in the low and middle latitudes, where the value tends to remain  $\leq 0.1$  percent for the same altitude region.

## 4. Diurnal Variations

- a. Because of a lack of sufficient numbers of comparable day and night data, no definite trend can be said to have been detected in the variability of the correction term as a function of diurnal period. Only in the subtropical summer data could such a comparison be made. This single comparison suggested a slightly larger value of correction term for nighttime data than for daytime data.
- b. When using data cells for which there has been a grouping across seasons, the value of the correction term for tropical, daytime data showed no significant difference from that for tropical nighttime data. The subtropical

data combined across seasons reflected the same diurnal differences previously discussed for the ungrouped summertime data for that latitude. No similar comparisons of seasonally grouped day and night data were possible for the other latitude belts because of insufficient data.

- c. For grouping across both season and latitude, the value of the correction term for altitudes below 90 km is slightly larger for the nighttime data than for the daytime data; i.e.,  $\leq 1.0$  percent compared with  $\leq 0.5$  percent.

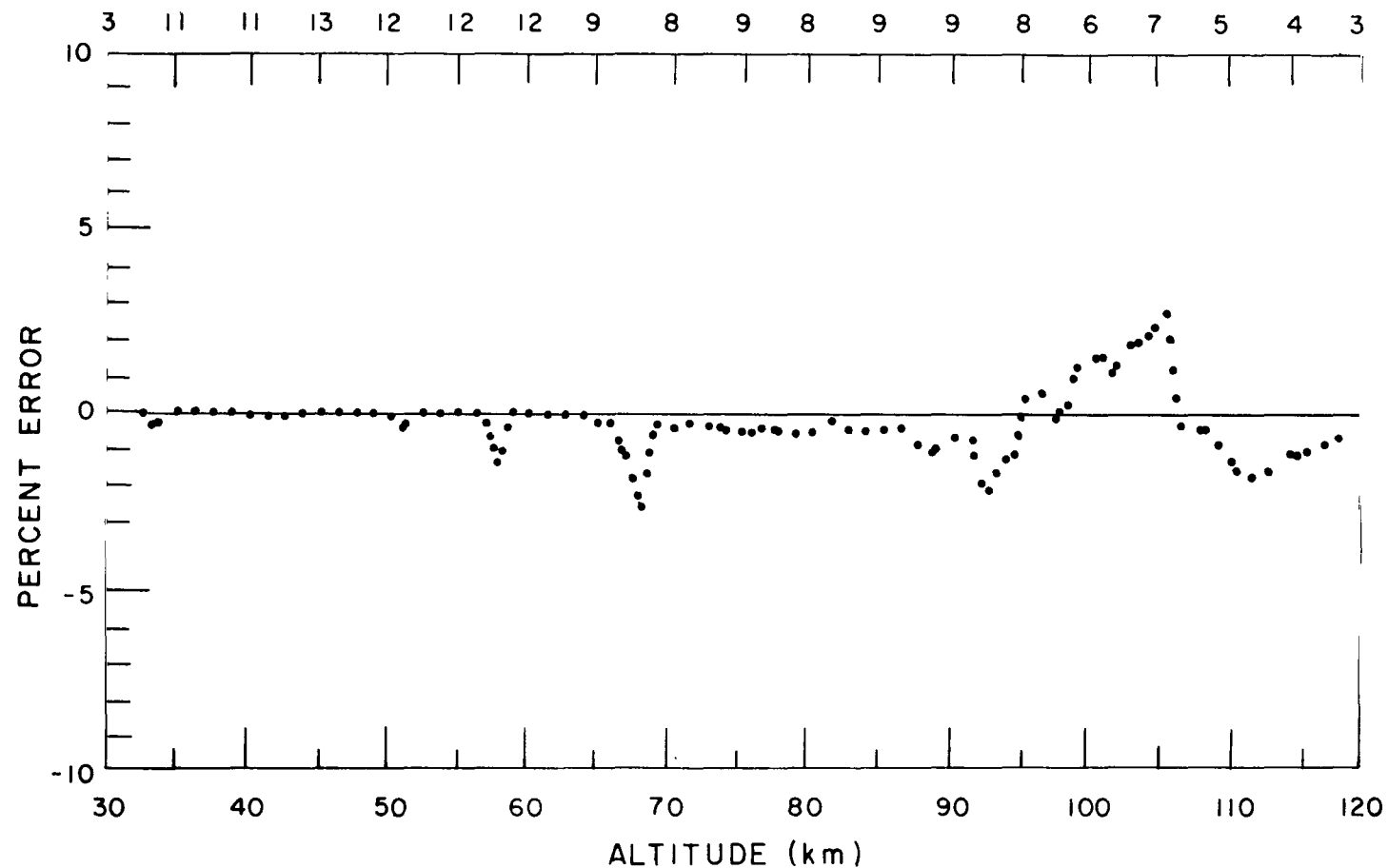
The observed time and space variations summarized above are based on analysis of the gross features of the numerical results. Within smaller altitude regions, values for the correction term showed one or more random negative excursions which are large compared with the remainder of that portion of the graph. A particular case in point is that illustrated by the graph for the tropical, summer, diurnal-mean data cell (see Figure 1). Sharp negative excursions of the correction-term value to  $-0.4$ ,  $-1.4$ , and  $-2.4$  percent are seen to exist at 51, 58, and 68 km, respectively, whereas in the remainder of the altitude region between 35 and 65 km the term has values of  $\leq 0.1$  percent. These appear to be the result of spurious density values at isolated altitudes and are most evident in data cells of small sample size. Consequently, these excursions have been largely disregarded in the search for general trends.

#### Analysis of the Covariance Term

For a better understanding of the factors influencing the variability of the covariance term, it is convenient to review the second term of the bracketed factor in Eq. (9). Of the three factors in this expression, the ratio  $\sigma\{\rho\}/\bar{\rho}$  as well as that of  $\sigma\{T\}/\bar{T}$  vary only slowly with altitude. These two ratios have values which are greater than zero and less than  $+1.0$  for all cases considered. The value of  $r\{\rho, T\}$  by definition may never exceed the range of  $-1.0$  to  $+1.0$ . The sign of the triple product is determined by the sign of  $r\{\rho, T\}$ , and the entire term vanishes when  $r\{\rho, T\}$  passes through zero.

A more detailed review of the computed, but unplotted values of  $\sigma\{\rho\}/\bar{\rho}$  and  $\sigma\{T\}/\bar{T}$ , shows that both quantities tend to increase with altitude. The first quantity ranges from as little as 0.05 or less at 30 km to 0.5 or more at 200 km. The second ranges from as little as 0.02 or less at 30 km to 0.4 or more at 200 km. Such changes with altitude are readily explained by a combination of greater relative variability in their parameters and increased measurement uncertainty of both  $\rho$  and  $T$  with increasing altitude.

NO. SAMPLES



TROPICAL

SUMMER

DIURNAL MEAN

Figure 1.- Percent contribution of the correction term to the mean pressure of the Buell gas law equation as a function of altitude

At any particular altitude, the values of both ratios tend to be smaller for homogeneous data than for heterogeneous data; i.e., smaller for data associated with a single latitude band, a single season, and a single diurnal period than for data which have not been segregated according to these variables. Because of these variations in the values of the two ratios, we might expect to find the values of the covariance or correction term to increase rather uniformly with increasing altitude and with increasing heterogeneity of other conditions of observation, provided that the value of  $r\{\rho, T\}$  were constant. The fact that the value of the correction term does not increase uniformly with altitude is due to a number of factors:

1. The value of  $\sigma\{\rho\}/\bar{\rho}$  does not increase smoothly with increasing altitude. Spurious values of density increase the value of  $\sigma\{\rho\}$  to a much greater extent than they influence the value of  $\bar{\rho}$ . Hence, particular altitudes or limited altitude regions occasionally have abnormally large values of  $\sigma\{\rho\}/\bar{\rho}$ .
2. Anomalous measured values of  $\rho$  at one altitude produce associated spurious computed values of  $T$  at another altitude. Thus, a large value for  $\sigma\{T\}/\bar{T}$  at a given altitude may be a consequence of a large value of  $\sigma\{\rho\}/\bar{\rho}$  at another altitude.
3. In addition, since single observations of  $\rho$  and  $T$  at any altitude are related by the gas law, a spuriously large value of  $\rho$  will have an associated spuriously small value of  $T$ , at that altitude. The converse also applies. This situation enhances the generation of the negative value of  $r\{\rho, T\}$  at the same altitude, and this value of  $r\{\rho, T\}$  tends to override the value which would otherwise be associated with that altitude region.
4. Investigations beyond the scope of this study suggest that various factors cause the value of  $r\{\rho, T\}$  to vary in a somewhat systematic manner with altitude, latitude, and possibly with season. It is sufficient to indicate at this point, however, that  $r\{\rho, T\}$  is far from being constant.

The relative influence of the factors  $\sigma\{\rho\}/\bar{\rho}$ ,  $\sigma\{T\}/\bar{T}$ , and  $r\{\rho, T\}$  on the values of the correction term depicted in Figure 1 are illustrated in Figure 2. It is apparent that the triple product of the three factors and the implicit relationships are such that spurious local values of density produce strong negative values in the altitude profile of the value of the correction term. Assuming that such spurious density values are not truly characteristic of the atmosphere but merely represent sampling fluctuations, it appears reasonable to disregard such random excursions in the graphs of the altitude dependence of the correction term.

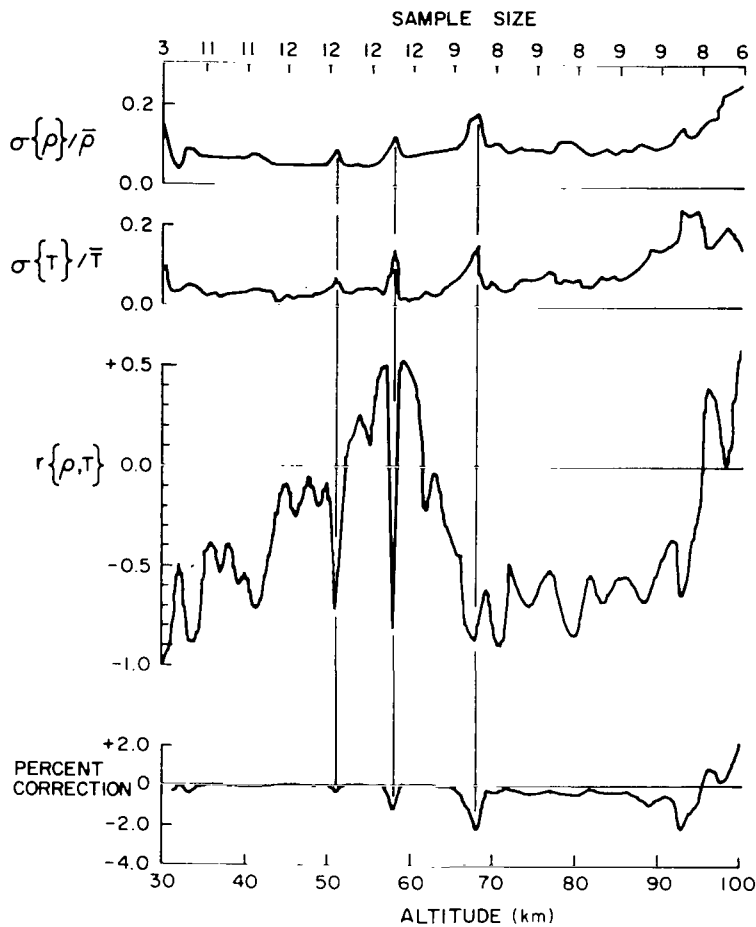


Figure 2.- Altitude profiles for the correction term value and each of the three factors which contribute to this value as determined for the tropical, summer, and diurnal-mean data cell

#### Summary of the Analysis of the Gas-Law Model

In summation it appears that the absolute magnitude of the correction term of the statistical form of the gas law increases with increasing altitude and with increasing latitude, but generally it remains below 1 percent for altitudes below 80 to 90 km, when a significant sample size exists. The value of the correction term seems to be greater in the winter than in the summer for high-latitude data, but no such variation is seen for low-latitude data. Time of day does not appear to influence strongly the value of the correction term in our limited data sample.

Over broad height intervals below 60 or 70 km the correction-term values for homogeneous data remain near 0.1 percent. This value is similar to that reported by Wood and Spreen (ref. 14) for homogeneous data at altitudes below 30 km.

For most model-atmosphere requirements at altitudes below 120 km, the value of the correction term which should be applied in computing mean pressure is usually small compared with other uncertainties in the models, and the application of this correction term may be omitted. Consequently, for altitudes below 120 km, the procedure commonly used to develop model atmospheres appears to be a valid one. Sophisticated models based on observed data, however, might well be based on calculations which include such a correction term, particularly for altitudes above 120 km.

### III. DISCUSSION OF RESULTS FOR THE STATISTICAL FORM OF THE HYDROSTATIC EQUATION

#### Description of the Graphical Data

The validity of the statistical model (Eq. 15) as applied to numerical data was determined by evaluating Eq. (16). This quantity was found to be highly variable with changes of one or two orders of magnitude between adjacent values accompanied by frequent change of sign. The unconnected dots in Figure 3 illustrate this variability for a typical data cell. This function is associated with the left ordinate of the graph which is designated PERCENT DIFFERENCE. Any computed values beyond the indicated range of the ordinate,  $\pm 100$  percent, have been truncated at those limits in the plotting procedure.

To improve the readability of this and similar graphs, only an envelope of the successive maxima and minima of the percent difference was plotted as a function of altitude. The graph of such an envelope for the same data cell depicted in Figure 3 is represented by the pair of dotted curves in Figure 4.

The series of + signs in each of Figures 3 and 4 represent the graph of  $\sigma\{p\}$  as a function of altitude. The ordinate for this graph is given at the right-hand side of the figure. The scale is logarithmic over the range  $10^2$  to  $10^{-4}$  nt/m<sup>2</sup> and the general linearity of the curve shows the near exponential height dependence of the statistic.

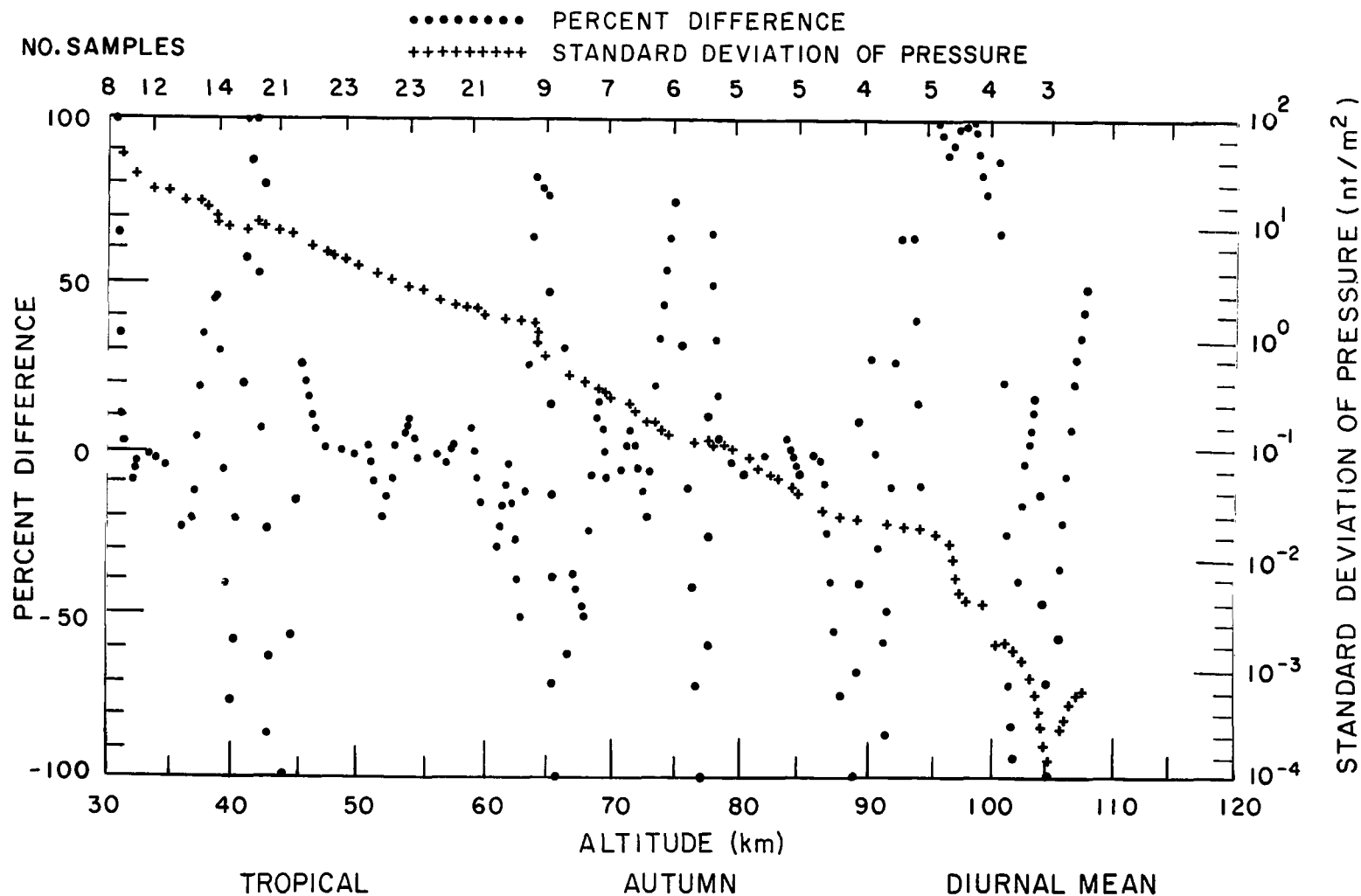


Figure 3.- Altitude profiles of the standard deviation of pressure and of the percent difference defined by Eq. (16) for the indicated latitude belt, season, and diurnal period

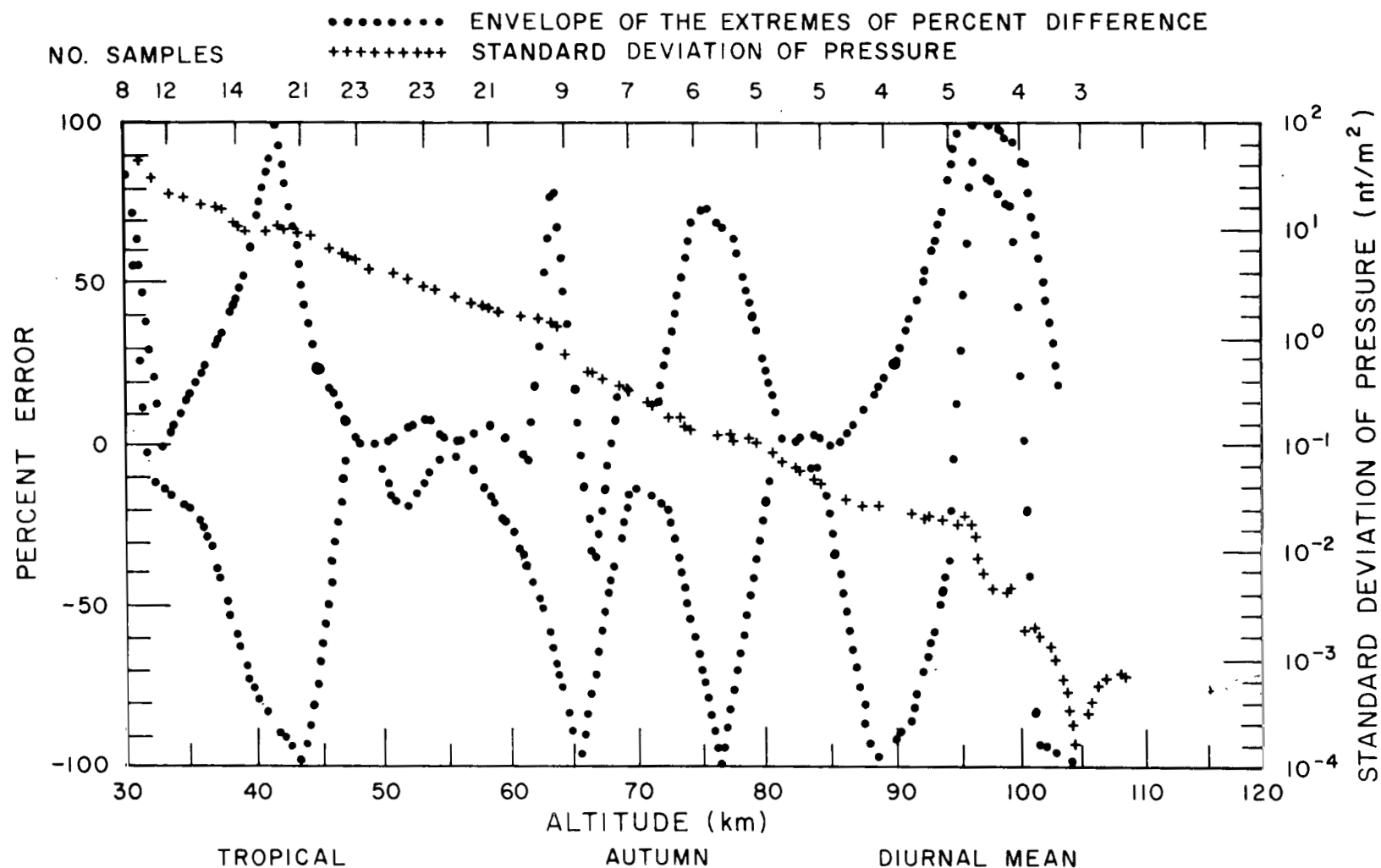


Figure 4.- Altitude profiles of the standard deviation of pressure and of the envelope of the extreme values for percent difference using the same data set as in Figure 3



## Interpretation of the Percent Difference Validity Test

A review of the results given in Figure 4 and in the many similar graphs depicting the same model for other data sets, as presented by Minzner and Morgenstern (ref. 11) suggests that the agreement between the two sides of the statistical model is rather poor. The truncation procedure used in the preparation of these graphs is such that in many instances the true difference is greater than the graphs suggest. However, it should be noted that the greatest departures occur in the regions where the curve of  $\sigma\{p\}$  shows rapid changes of slope, resulting in poor agreement with the model. In height regions where the profile of  $\sigma\{p\}$  is nearly linear on this graph, i.e., the derivative is nearly constant such as the 45 to 60 km interval, the agreement is much more favorable.

A better indication of the relative smoothness of the individual terms in this model is shown by the curves in Figure 5. The crosses represent the values of the derivative on a logarithmic scale\* while the solid line in Figure 5 represents the values of the right-hand side of Eq. (15). A visual comparison of these curves shows the greater variability in the derivative term. However, both curves are reasonably smooth and in relative agreement over that portion of the altitude range for which the sample size exceeds 20.

The influence of greater sample size is illustrated by the results shown in Figure 6 for a more populous data cell. The region of reasonably good agreement extends over a much larger altitude interval in this instance than in Figure 5. Some relatively large differences are observed in Figure 6, primarily in the region of rapid decrease of sample size, and one positive value of the derivative is found in the same region.

Figures 5 and 6 both show that neither side of Eq. (15) represents a very smooth function of altitude. The derivative term is highly sensitive to local changes in slope of the  $\sigma\{p\}$  profile produced by measurement uncertainties in the data. This suggests that further smoothing of the data is desirable for evaluation of the differential-equation model in the form of Eq. (15). Section IV contains a description of an alternate form of the model which provides implicit smoothing of the data.

\*Because  $\sigma\{p\}$  is a decreasing function with altitude, the derivative generally is negative. Hence the absolute values have been plotted.

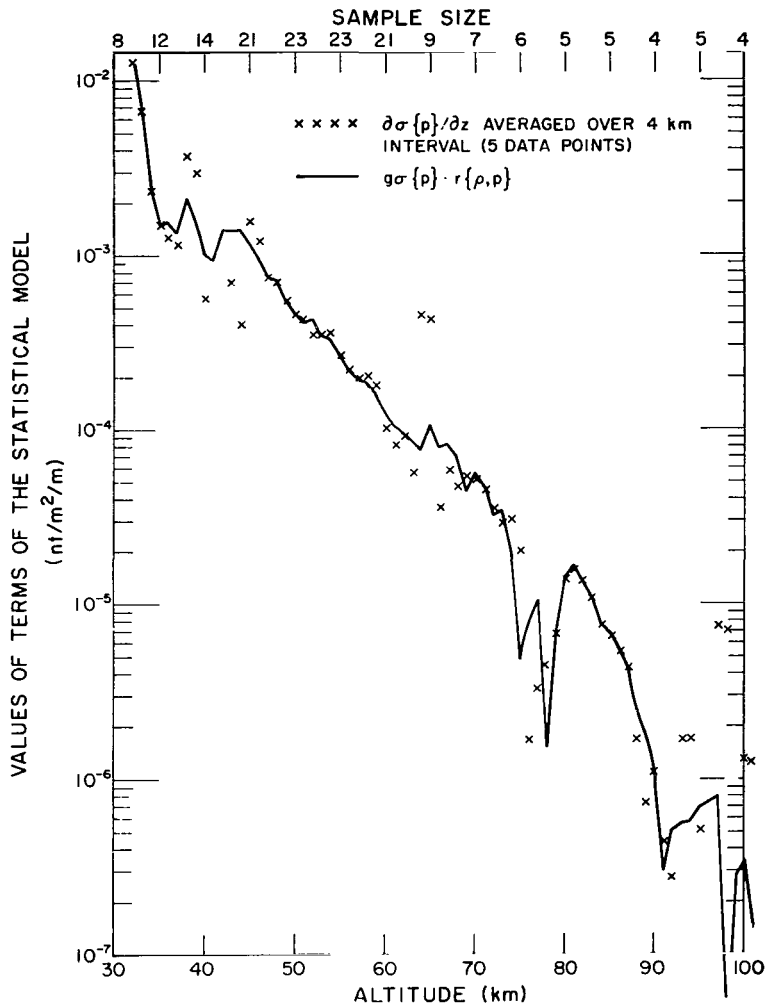


Figure 5.- Altitude profiles of the right and left sides of Eq. (15) evaluated for the tropical, autumn, diurnal-mean data cell

#### Summary on the Degree of Validity

The analysis of this model suggests that the number of soundings available for use in the current study generally is inadequate to establish the validity of the model. This is a consequence of the sensitivity of the statistical variables to sampling fluctuations in the data. The model yields the best results for those altitude regions containing the largest sample sizes.

#### IV. REVISION OF STATISTICAL HYDROSTATIC EQUATION MODEL

The results of the previous section have shown that the statistical model of Eq. (15) is highly sensitive to random sampling fluctuations of the meteorological variables. The nearly opposite character of differentiation and integration suggests that an integral form of the hydrostatic-equation model may be developed to overcome the limitations of the differential form. Equation (15) can be integrated with respect to altitude to yield

$$\sigma\{p\}_z = \sigma\{p\}_o - \int_{z_o}^z g \cdot \sigma\{\rho\} \cdot r\{\rho, p\} dz \quad (18)$$

where the subscript (<sub>o</sub>) refers to the uppermost altitude of the height interval of integration. The quantity  $\sigma\{p\}_o$  is the standard deviation of pressure at height  $z_o$ . This model can be simplified further if the acceleration of gravity is assumed to be constant. The validity of this assumption is examined in greater detail in Section V where it is established that the resulting error is not significant.

Equation (18) with ( $g$ ) assumed constant may be evaluated by use of an appropriate numerical integration technique. Because  $\sigma\{\rho\}$  is nearly an exponential function of height, a logarithmic integration formula is desirable. Minzner (ref. 15) has tested several simple integration techniques on atmospheric variables and found that the logarithmic trapezoidal rule yielded satisfactory results when applied to density profiles. Application of this rule to Eq. (18) produces

$$\sigma\{p\}_i = \sigma\{p\}_o - g \sum_{j=1}^{j=i} \frac{(z_j - z_{j-1}) \cdot (Q_j - Q_{j-1})}{\ln (Q_j / Q_{j-1})} \quad (19)$$

where

$$Q = \sigma\{\rho\} \cdot r\{\rho, p\}$$

and the subscript ( $i$ ) refers to the number of integer kilometer increments below  $z_o$ . A more detailed discussion of this integration method is given in Appendix A of this report.

Equation (18) as approximated by Eq. (19) was evaluated numerically with the same set of data used to develop Figure 6. The observed value of  $\sigma\{p\}$  at  $z_o$  is used as an estimate of  $\sigma\{p\}_o$ . The effect of sampling errors in  $\sigma\{p\}_o$  on the values of  $\sigma\{p\}_i$  as derived for the right-hand expression is dis-

cussed further in Appendix A. A comparison curve, the altitude profile of  $\sigma\{p\}$  was calculated directly from observed values of atmospheric pressure. Figure 7 shows the results of these computations. These curves are significantly smoother than the results from the differential-equation model shown in Figure 6. A comparison of the two curves in Figure 7 shows that the differences are smaller than in Figure 6, and now tend to be systematic in character. The discontinuities still exhibited by these curves generally are associated with sharp changes in the sample size of the data set.

The validity of this model can be examined in a manner similar to that used for the differential-equation model, namely:

$$\text{percentage difference} = 100 \left[ \frac{\sigma\{p\}_i - \sigma\{p\}}{\sigma\{p\}} \right] \quad (20)$$

(The direction of the difference in the numerator of Eq. (20) has been reversed to be consistent with the implicit signs in Eq. (16) introduced by negative slopes.) The altitude profile of Eq. (20) for the same set of data used in Figures 6 and 7 is shown by the dashed curve in Figure 8. The percent difference in this graph shows a maximum of 60 percent error with large segments of the profile indicating less than a 15 percent difference. A direct comparison of these results with those for the differential equation model also is provided by the solid curve in Figure 8. The departures in this latter case are seen to be substantially greater. It is apparent that the integral version of the model provides a more suitable basis than the differential model for investigating the existence of latitudinal, seasonal, or diurnal variations in the validity of the statistical model.

## V. CONCLUSIONS

The objective of this study has been to evaluate the validity of two models for relating the statistics of atmospheric pressure, temperature, and density. These models were applied to data assembled from 437 upper-air soundings for the region 30 to 200 km. The results of these calculations showed that the covariance term of Eq. (7) was generally in the range  $\pm 1.0$  percent of the mean pressure for the altitudes 30 to 60 km. In this height interval the covariance was largest at upper altitudes, in arctic latitudes, and during winter months. Above 60 km the covariance term exceeded  $\pm 1$  percent in many cases but these results are less reliable because of the more limited number of sounding available for analysis, particularly at the higher

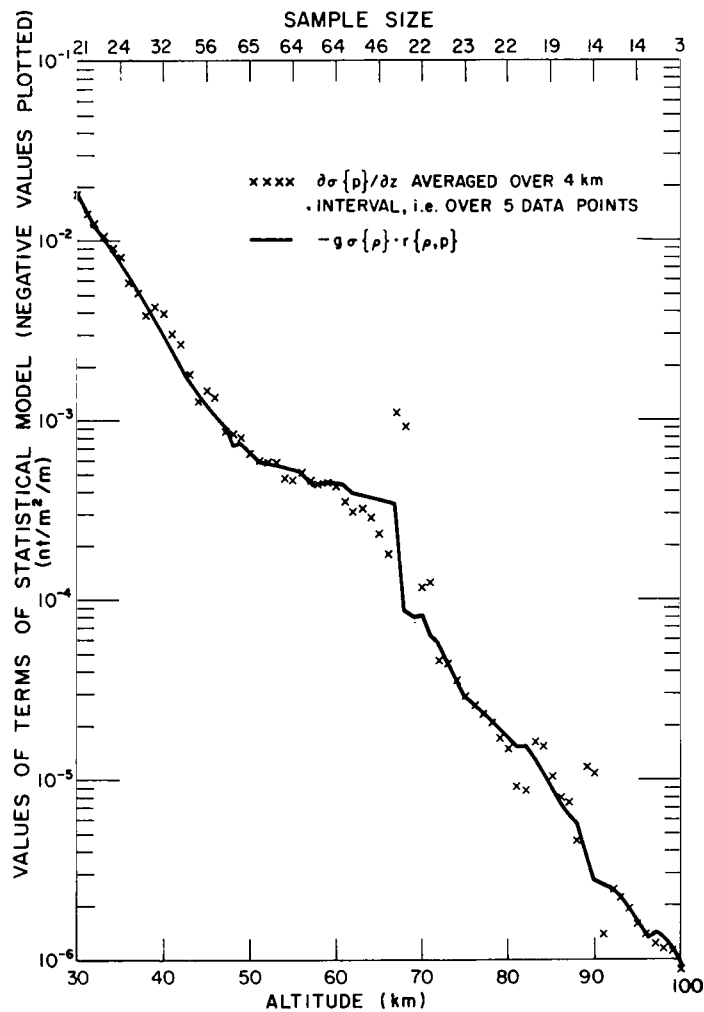


Figure 6.- Altitude profiles of the right and left sides of the differential model of Eq. (15) evaluated for the subtropical, autumn, diurnal-mean data cell

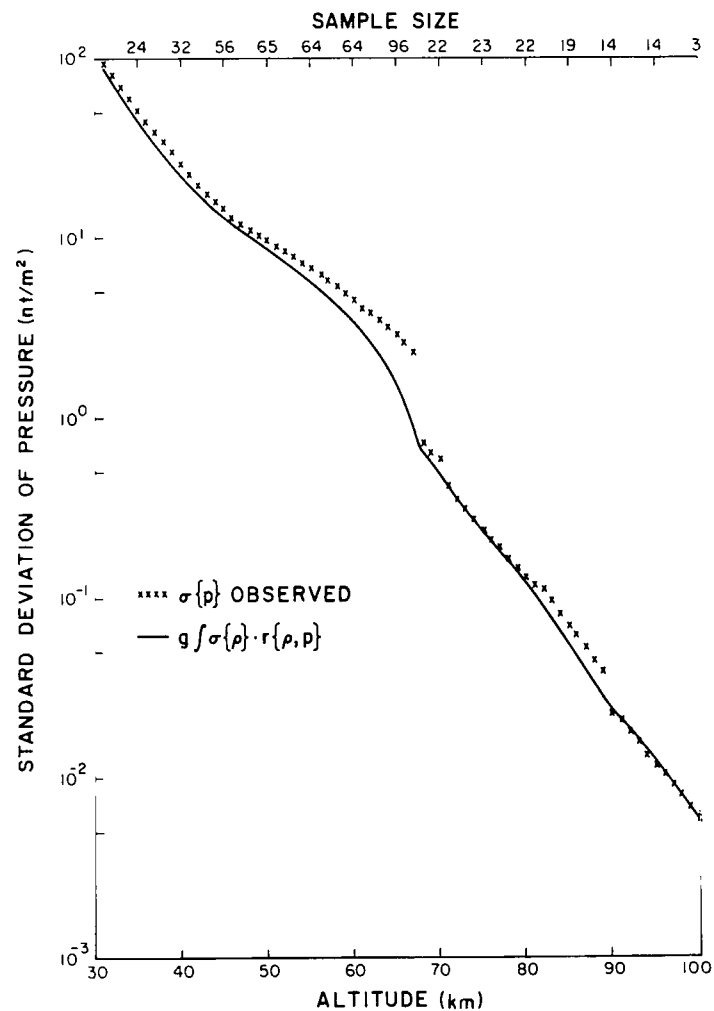


Figure 7.- Altitude profile of the standard deviation of pressure compared with the same quantity inferred from the integral of Eq. (18), using the same data employed in Figure 6

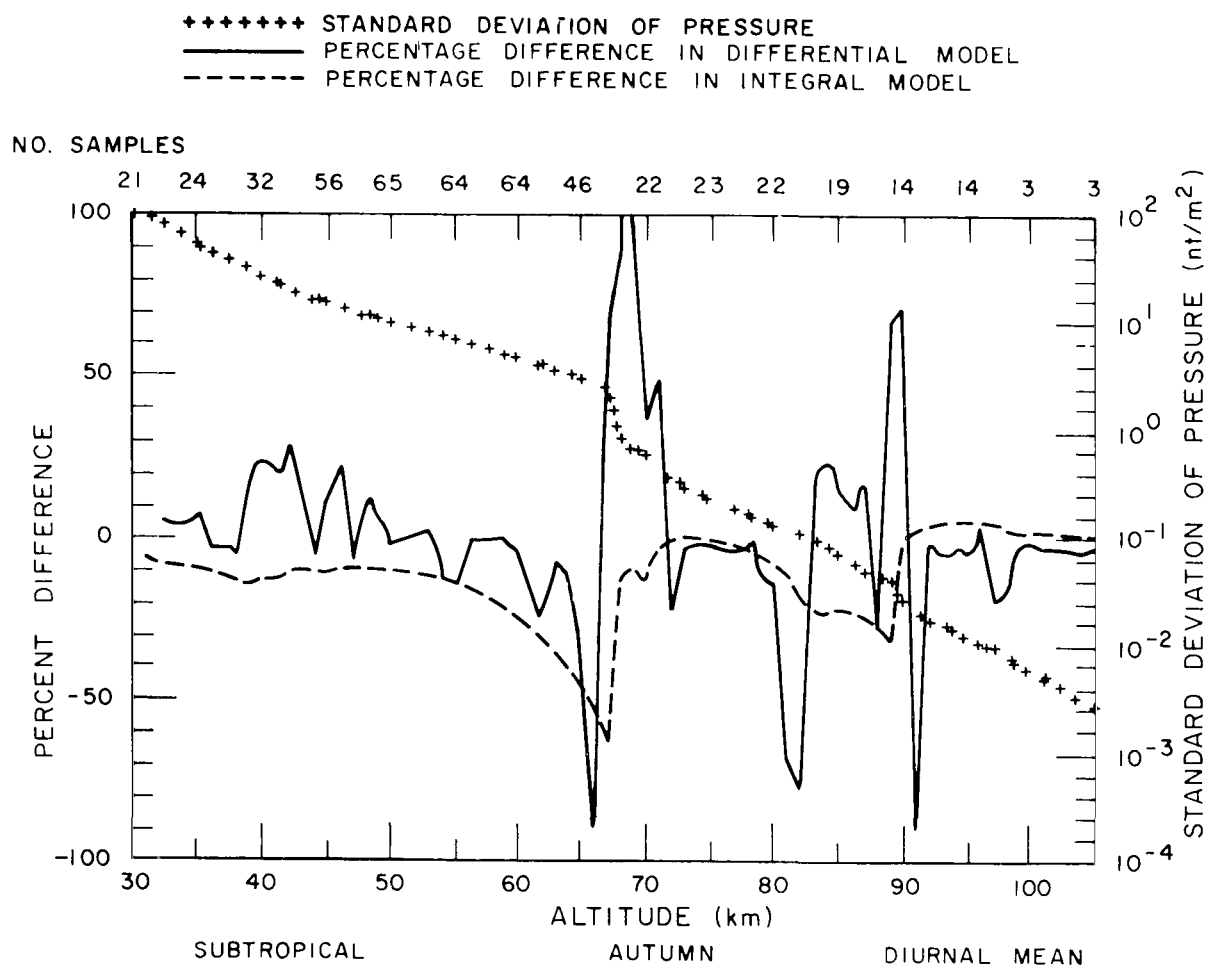


Figure 8.- Comparison between percent departure for the differential-equation model (solid line) and the model expressed by Equation (18) in integral form (dashed line) - corresponding values of standard deviation of pressure calculated directly from pressure data (crosses)

latitudes. Because of a lack of sufficient comparable day and night data, no definite trend can be said to have been detected in the variability of the covariance term as a function of the diurnal period.

The analysis of the model given by Eq. (15) suggests that the number of soundings available for use in the current study generally is inadequate to establish the validity of the model. This is a consequence of the sensitivity of the statistical variables to sampling fluctuations in the data. The model yields the best results for those altitude regions containing the largest sample sizes. Because of these limitations, a revision of the basic model has been proposed changing it from a differential equation into an integral form. The revised model was evaluated for a single case by means of a logarithmic trapezoidal integration scheme. A comparison of these results with those from the original model suggests that the integral form provides a more suitable basis for future investigations of the existence of latitudinal, seasonal, or diurnal variations in the validity of the model.

Gravity variations as a function of altitude and of latitude were considered in the initial processing of the individual soundings. In the subsequent analysis of the data, the results of many soundings were grouped according to geometric altitude both within a latitude band, and across latitude bands. This grouping at identical geometric altitudes across latitude bands is now seen to be a less desirable procedure, and has perhaps led to larger values of standard deviations of density and pressure than would have resulted if the data had been grouped according to equal values of geopotential (refs. 16, 17).

## APPENDIX A

### NUMERICAL EVALUATION PROCEDURES

The purpose of this appendix is to discuss qualitatively how the magnitude of the uncertainties in the model values for  $\sigma\{p\}$  are influenced by the choices in each of two procedures in the evaluation of the expression:

$$\sigma\{p\} = \sigma\{p\}_0 - \int_{z_0}^z \sigma\{\rho\} \cdot r\{\rho, p\} dz \quad (A-1)$$

The first of these procedures is the numerical evaluation of the integral term by means of a quadrature formula. Several quadrature formulas were considered from which the logarithmic trapezoidal rule was selected as providing a satisfactory approximation to the actual integral. The merits of some alternate choices are discussed later. The uncertainty which would be introduced into the value of  $\sigma\{p\}$  by selecting a less suitable quadrature formula is small, however, compared with the uncertainty introduced into  $\sigma\{p\}$  by the observational uncertainties in  $\sigma\{\rho\} \cdot r\{\rho, p\}$ .

An even greater uncertainty is introduced into  $\sigma\{p\}$ , however, by a poor choice in the second procedural item, i.e., that dealing with the direction of integration, upward or downward. It will be shown that only downward integration yields acceptable values of percent uncertainty over the entire region of integration, although upward integration as implied by Eq. (A-1) may, in some instances, be satisfactory for a very limited region at the lower end of the range of integration.

With upward integration the model values of  $\sigma\{p\}$  are determined as a small difference between two large quantities, an intuitively undesirable procedure. It will be shown that in such a situation, the percent uncertainty propagated into the difference  $\sigma\{p\}$  is an *amplified* weighted average of the percent uncertainties of both the terms comprising the difference. This propagated uncertainty in  $\sigma\{p\}$  is never less than the percent uncertainty of the minuend, which is the integration constant, and grows without bounds as  $z$  increases.\*

With downward integration, however, the model values of  $\sigma\{p\}$  are determined by a summation operation as in Eq. (A-2), which comes directly from Eq. (A-1):

---

\*Both lower-case and upper case forms of  $Z$  used interchangeably in this appendix signify geometric height.



$$\sigma\{p\} = \sigma\{p\}_0 + \int_z^{z_0} \sigma\{p\} \cdot r\{p, p\} dz \quad (A-2)$$

In such an operation, it can be shown that the percent uncertainty in the sum, is a *normal* unamplified weighted average of the percent uncertainties of the addends, and consequently *never* exceeds the percent uncertainty of the larger addend. This will be seen to be the integral term for all but the first few kilometers of the range of integration.

The weighting feature operates so as to minimize the effect of the percent uncertainties of small quantities involved in the sums or differences, even when these small quantities have very large uncertainties. This feature is most apparent and particularly beneficial in the summation representing downward integration, where the magnitude of the constant of integration  $\sigma\{p\}_0$  is very small compared with that of the integral term over most of the range of an extended integration, but where the percent uncertainty of  $\sigma\{p\}_0$  is large compared with that of the integral term. This large percent uncertainty in the integration constant is effectively eliminated from the uncertainty in model values of  $\sigma\{p\}$  by the weighting feature.

Both the weighting and amplification features which will be demonstrated analytically in the next section, favor the downward direction of integration. This conclusion is readily substantiated from an analysis of the error expressions associated with each of Eqs. (A-1) and (A-2).

#### ERROR ANALYSIS

To simplify the form of the expressions showing the error propagation into  $\sigma\{p\}$  within each of Eqs. (A-1) and (A-2), it is desirable to simplify the symbolic notation of the terms of these equations prior to writing the error expressions. Thus, the quantity being computed,  $\sigma\{p\}$ , is changed to  $Q$ ; the constant of integration  $\sigma\{p\}_0$  is changed to  $C$ , and the entire integral term is designated by  $I$ . Then, using the Gaussian method we may relate the absolute uncertainties  $\delta Q$ ,  $\delta C$ , and  $\delta I$  in  $Q$ ,  $C$ , and  $I$  respectively, through partial derivatives as follows:

$$\delta Q = \sqrt{\left(\frac{\partial Q}{\partial C} \cdot \delta C\right)^2 + \left(\frac{\partial Q}{\partial I} \cdot \delta I\right)^2} \quad (A-3)$$

Because the variables C and I in Eqs. (A-1) and (A-2) appear only in the first power, in separate terms, and without coefficients, it follows that:

$$\delta Q = \sqrt{(\delta C)^2 + (\delta I)^2} \quad (A-4)$$

Designating percent uncertainties in Q, C, and I as PUQ, PUC, and PUI, it follows that:

$$\delta C = C \cdot \frac{\delta C}{C} = \frac{1}{100} \cdot C \cdot PUC \quad (A-5)$$

and

$$\delta I = I \cdot \frac{\delta I}{I} = \frac{1}{100} \cdot I \cdot PUI \quad (A-6)$$

These forms are equally correct when applied to the percent uncertainties of both Eqs. (A-1) and (A-2). The conversion of  $\delta Q$  to a form involving PUQ, however, differs in the two cases, and we have:

$$\delta Q = Q \cdot \frac{\delta Q}{Q} = \frac{1}{100} \cdot (C-I) \cdot PUQ \quad (A-7)$$

applicable to Eq. (A-1), and:

$$\delta Q = Q \cdot \frac{\delta Q}{Q} = \frac{1}{100} \cdot (C+I) \cdot PUQ \quad (A-8)$$

applicable to Eq. (A-2).

Combining Eqs. (A-4), (A-5), (A-6), and (A-7) into one equation, and then combining Eqs. (A-4), (A-5), (A-6), and (A-8) into another equation we obtain:

$$PUQ_1 = \sqrt{\frac{(C_1 \cdot PUC_1)^2 + (I_1 \cdot PUI_1)^2}{C_1 - I_1}} \quad (A-9)$$

for upward integration, and:

$$PUQ_2 = \sqrt{\frac{(C_2 \cdot PUC_2)^2 + (I_2 \cdot PUI_2)^2}{C_2 + I_2}} \quad (A-10)$$

for downward integration. The subscript 1 added to the symbols Q, C, and I in Eq. (A-9) designates the particular values of these quantities applicable to Eq. (A-1) for upward integration. The subscript 2 employed similarly in Eq. (A-10) designates the particular values applicable to Eq. (A-2) for downward integration.

#### NUMERICAL VALUES

In order to investigate the error amplification as well as the weighting effects of Eqs. (A-9) and (A-10) with some degree of quantitateness, it is necessary to have some reasonable estimates of the values of  $C_1$ ,  $C_2$ ,  $I_1$  and  $I_2$ , as well as the uncertainties in  $C_1$  and  $C_2$ . These all follow from an estimate of the altitude profile of  $Q \equiv \sigma\{p\}$  and its uncertainty. The values associated with the lower and upper ends of such a profile serve respectively as reasonable values for the constants  $C_1$  and  $C_2$  and their uncertainties. With these quantities we can derive estimates of the altitude profiles of  $I_1$  and  $I_2$  through the following relationships stemming directly from Eqs. (A-1) and (A-2) respectively:

$$I_1 = C_1 - Q \quad (A-11)$$

$$I_2 = Q - C_2 \quad (A-12)$$

The number of upper-atmosphere observations available for analysis falls off rapidly with increasing altitude. The decrease occurs nearly stepwise in three height regions: (1) in the vicinity of 30 kilometers, (2) in the vicinity of 50 kilometers, and (3) in the vicinity of 90 kilometers. At heights up to about 28 kilometers, the values of atmospheric pressure

and density, as well as their respective standard deviations,  $\sigma\{p\}$  and  $\sigma\{\rho\}$  are reasonably well known from many thousands of observations. For purposes of this discussion, the value of  $\sigma\{p\}$  at an altitude of 28 kilometers, the low limit of the altitude profile is taken to be  $1.45 \times 10^2 \text{ nt m}^{-2}$ , with an uncertainty of  $\pm 6$  percent. The same percent uncertainty is assumed for the value of  $\sigma\{\rho\}$  which is taken to be  $2.08 \times 10^{-3} \text{ kg m}^{-3}$  at this altitude. The 28-kilometer value of  $\sigma\{p\}$  and its uncertainty have been adopted as  $C_1$  and  $\delta C_1$  respectively.

Above 90 kilometers height, the number of atmospheric soundings decreases rapidly with increasing height. Between 90 and 108 kilometers, the available data sample for the study reported in the main body of this paper for any particular height level, summed over all observation sites, decreased from 84 to 37 samples. For this latter altitude, the value of  $\sigma\{p\}$  was calculated to be  $2.7 \times 10^{-3} \text{ nt m}^{-2}$ , while the value of  $\sigma\{\rho\}$  was calculated to be  $3.69 \times 10^{-1} \text{ kg m}^{-3}$  (ref. 11). This value of  $\sigma\{p\}$  has been adopted for the upper limit, of the altitude profile of  $\sigma\{p\}$ , where the percent uncertainties of both  $\sigma\{p\}$  and  $\sigma\{\rho\}$  are assumed to be  $\pm 100$  percent. This value of  $\sigma\{p\}$  and its uncertainty have been adopted for  $C_2$  and  $\delta C_2$  respectively. The 108-kilometer value of  $\sigma\{p\}$  is seen to be five orders of magnitude smaller than the adopted 28-kilometer value of  $1.45 \times 10^2 \text{ nt m}^{-2}$ . It is apparent that  $\sigma\{p\}$  or  $Q$  must vary approximately exponentially, i.e., in the manner of  $KC^{-\alpha Z}$ , between these two altitudes. Using the cited end-point values of  $Q$  to define the function, it can be shown that the value of  $K$  is  $6.504 \times 10^3 \text{ nt m}^{-3}$ , and that of  $A$  is  $1.359 \times 10^{-4} \text{ m}^{-1}$ . The value of  $\sigma\{\rho\}$  is assumed to approximate a similar function  $ke^{-\alpha Z}$  such that the cited end points imply a value of  $9.592 \times 10^{-2} \text{ kg m}^{-3}$  for  $k$ , and a value of  $1.368 \times 10^{-4} \text{ m}^{-1}$  for  $\alpha$ .

#### UPWARD INTEGRATION

With the value of  $C_1$  and the altitude profile of  $Z$  established, Eq. (A-11) yields the altitude profile of  $I_1$ , an approximation of which is shown in Figure A-1. For the sake of simplicity, no uncertainty band has been indicated for this quantity although the uncertainty in  $I$  is discussed below. The adopted value of  $C_1$  is also shown in this figure, but in this case an uncertainty band of  $\pm 6$  percent is given. The value of  $C_1$  and its uncertainty band are given by three lines  $C_{1.1}$ ,  $C_{1.2}$ , and  $C_{1.3}$ , where  $C_{1.2}$  represents the adopted value of  $1.45 \times 10^2 \text{ nt m}^{-2}$ , and where  $C_{1.1}$  and  $C_{1.3}$  represent, respectively, the  $+6$  percent and  $-6$  percent departures from the adopted value. It is apparent from the figure that except for the very lowest portion of the range of integration, the value of  $I_1$  is of the same order of magnitude as the value of  $C_1$ .

For altitudes above the lowest 4 kilometers of the range of integration, the value of  $I_1$  is greater than one half the value of  $C_1$ . Thus, for upward integration, it is apparent that except for the lowest altitude within the range of the integration, the magnitude of  $C_1$  and  $I_1$  are such that their percent uncertainties both contribute significantly to  $PUQ_1$ , as expressed by Eq. (A-9). For these altitudes, the relative magnitude of the two terms under the square-root sign depends primarily on the relative magnitudes of the percent uncertainties.

At  $Z_0$ , the initial altitude,  $I_1$  is zero and Eq. (A-9) reduces to:

$$PUQ_1 = \frac{\sqrt{(C_1 \cdot PUC_1)^2}}{C_1} = PUC_1 \quad (A-13)$$

As  $Z$  increases above  $Z_0$ ,  $I_1$  increases rapidly. At the same time, the growing value of  $(I_1 \cdot PUI_1)^2$  increases the value of the numerator of Eq. (A-9) to some value greater than  $\sqrt{(C_1 \cdot PUC_1)^2}$ , while the growing value of  $I_1$  decreases the value of the denominator to some value less than  $C_1$ . The two effects occurring simultaneously cause the value of  $PUQ_1$  to increase rapidly from its minimum value of  $PUC_1$ . At an altitude of about 20 kilometers above the bottom of the range of integration, where  $I_1$  approaches a value of about 0.9 of  $C_1$ , the value of  $PUQ_1$  becomes about 20 times that of  $PUC_1$ . As the integration proceeds to even greater altitudes above the initial level, the value of  $PUQ_1$  approaches infinity as  $(C_1 - I_1)$  approaches zero, essentially independent of the values of  $PUC_1$  and  $PUI_1$ . It is apparent from Figure A-1 that for a  $\pm 6$  percent uncertainty in  $C_1$  and no uncertainty in  $I_1$ , the value of  $(C_1 - I_1)$ , and, hence that of  $Q_1$  could become zero at an altitude  $Z_x$  as low as about 53 kilometers. At greater altitudes, the values of  $Q$  would be meaningless. An uncertainty band of  $\pm 6$  percent associated with  $I_1$  would expand the point  $Z_x$  to a region extending from a lower limit of about 43 km to the top of the range of integration, 108 km. Within this region, the model value of  $Q_1$  would be meaningless.

From this analysis, it is apparent that upward integration yields reasonable values of  $Q_1$  and  $PUQ_1$  only at altitudes very close to the reference level.

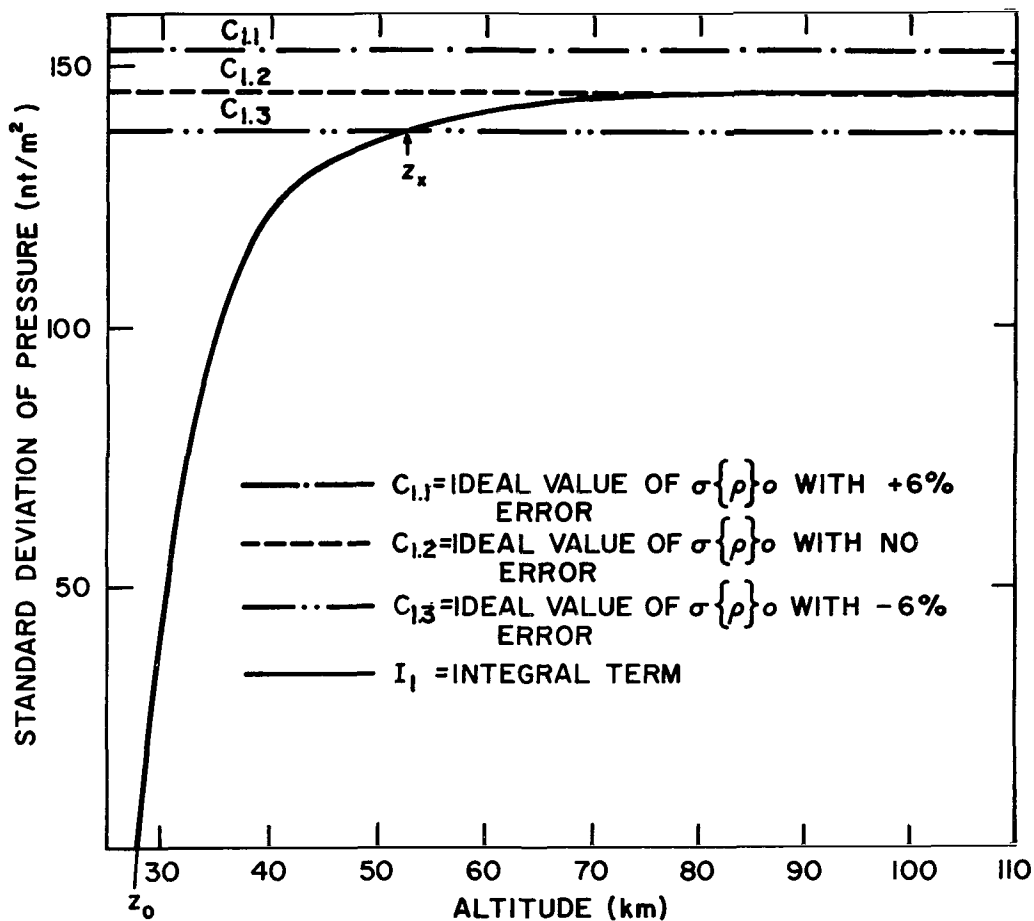


Figure A-1.- Relative values of the two terms of Eq. (A-1) as a function of altitude for upward integration from altitude  $z_0$

#### DOWNWARD INTEGRATION

The introduction of the value of the integration constant  $C_2$ , as well as the estimated altitude profile of  $Q$  into Eq. (A-12) yields an estimate of the altitude profile of  $I_2$ , the integral term associated with downward integration. An approximation of this quantity is depicted in Figure A-2. As in the case of  $I_1$ , simplicity precludes the depicting of an uncertainty band for  $I_2$ . For downward integration, from high to lower altitudes, the value of the integration constant  $C_2$  is very small compared with the value of  $I_2$  for much of the range of integration. The adopted value of  $C_2 = 2.7 \times 10^{-3} \text{ nt m}^{-2}$  with an assumed uncertainty band of  $\pm 100$  percent, if drawn to scale in Figure A-2,

could not be distinguished from the abscissa of the graph. Though not apparent from the graph, it may be stated that the value of  $I_2$  grows from zero to about ten times the value of  $C_2$  as the altitude decreases about 18 km from  $Z_0$ . From this point, the value of  $I_2$  continues to grow by a factor of about 10 for each successive 17-kilometer decrement in  $Z$  included within the integral. From this information, one may show that  $C_2$  is very small compared with  $I_2$  for all but the upper 20 to 30 kilometers of the range of integration. Thus, as the increasing range of altitudes encompassed by the integral becomes greater than 30 km, the contribution of  $PUC_2$  to  $PUQ_2$  through Eq. (A-10) becomes negligible even for an uncertainty in  $C_2$  as large as 100 percent.

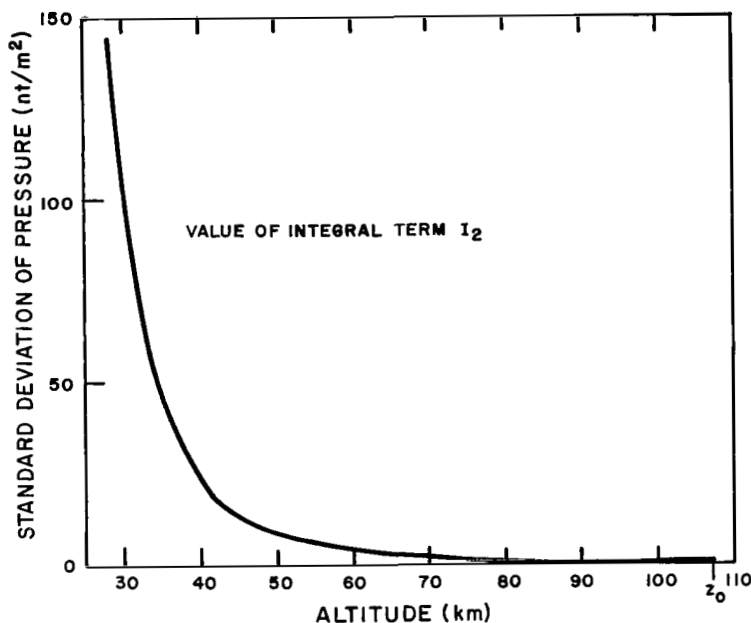


Figure A-2.- Values of the integral term of Eq. (A-2) as a function of altitude for downward integration from altitude  $z_0$

For this situation,  $(Z_0 - Z) > 30$  kilometers, Eq. (A-10) reduces essentially to:

$$PUQ_2 \cong \frac{\sqrt{(I_2 \cdot PUI_2)^2}}{I_2} = PUI_2 \quad (A-14)$$

At altitude  $Z_0$ , where  $I_2$  is zero, Eq. (A-10) reduces exactly to:

$$PUQ_2 = \frac{\sqrt{(C_2 \cdot PUC_2)^2}}{C_2} = PUC_2 \quad (A-15)$$

so that  $PUQ_2 = PUC_2$ , which is  $\pm 100$  percent for the adopted conditions. For altitudes within the upper 30 kilometers of integration, the uncertainty  $PUQ_2$  decreases from a maximum of  $PUC_2$  at  $Z_0$  toward the value of  $PUI_2$  as the altitude decreases from  $Z_0$ . Thus, Eq. (A-10) does not explode for any values of  $Z$ , and reasonable values of uncertainty of  $Q$  are obtained for the entire range of integration.

Obviously, if only one direction of integration is to be selected, downward integration is to be preferred over upward integration. If the value of  $PUI_2$  at 28 km altitude from downward integration is greater than  $PUC_1$ , upward integration may possibly yield a slightly more precise value of  $Q$  in the immediate vicinity of 28 km. The uncertainty of such a value of  $Q$  will, however, rapidly grow to unacceptable values if this upward integration process is carried out for more than a few kilometers.

#### QUADRATURE FORMULA

A somewhat secondary but necessary consideration effecting the overall uncertainty of the model values of  $\sigma\{p\}$  involves the selection of a quadrature formula to evaluate the integral term of Eqs. (A-1) and (A-2). The selected quadrature formula serves as the basis for the development of an uncertainty expression for the integral term. The reason for designating the selection of a quadrature formula as a secondary consideration is due to the fact that while different normally acceptable quadrature formulae approximate the actual integral with varying degrees of accuracy, the error introduced by the poorest of these approximations is very small compared with other uncertainties. Three relatively simple formulas which have been considered are: (1) the linear trapezoidal rule, (2) the logarithmic trapezoidal rule, and (3) Simson's rule. Minzner (ref. 15) has shown the logarithmic trapezoidal rule to be a good approximation of the definite integral for any function whose logarithm is nearly a linear function of the independent variable. Since the integrals  $I_1$  and  $I_2$  were both shown to meet this condition, the logarithmic trapezoidal rule has been adopted. Using this rule, we may rewrite Eq. (A-1) as well as Eq. (A-2) as:



$$\sigma\{p\}_i = \sigma\{p\}_o - g \sum_{j=1}^{j=i} \frac{(z_j - z_{j-1}) \cdot (v_j - v_{j-1})}{\ln(v_j/v_{j-1})} \quad (\text{A-16})$$

where

$$g = 9.80665 \text{ m sec}^{-2},$$

$z$  = height in meters,

$$V = \sigma\{p\} \cdot r\{p, p\},$$

$i$  = the number of increments included in the quadrature procedure thereby involving a total of  $(i + 1)$  altitudes.

With downward integration, the value of  $(V_j - V_{j-1})$  is positive, the value of  $z_{j-1}$  is greater than  $z_j$ , such that  $(z_j - z_{j-1})$  is negative, and this negative sign coupled with the negative sign of the summation term effectively makes  $\sigma\{p\}_i$  equal to the sum of two positive terms. The expression resulting from Simpson's rule would probably yield a slightly better approximation to the actual integral of Eq. (A-2) than that resulting from the logarithmic trapezoidal rule as shown in Eq. (A-16), but at the expense of considerably more complication. The linear trapezoidal rule would yield a somewhat poorer approximation, particularly in cases where the data points are distributed nonuniformly with altitude. The added uncertainty introduced into  $\sigma\{p\}$  by the poorest of these three quadrature formulas would be small, however, compared with the uncertainty which is propagated into  $\sigma\{p\}$  through the observational errors in the constant of integration and in the combined variable  $V$ , both of which enter into any quadrature formula that may be used to express  $I$ .

The precise form of the equation used to express the uncertainty of the integral term depends directly upon the particular quadrature formula used, and while the form of the uncertainty expression related to each of the several quadrature formulae differs extensively, one from the other, the value of the computed uncertainty  $\delta I$  for any common set of conditions is not apt to differ greatly regardless of the form of the uncertainty equation from which it is computed.

Again, the Gaussian method serves as the basis for the generation of the uncertainty expression, such that  $\delta I$  the absolute uncertainty in the integral term is given by:

$$\delta I = \sqrt{\sum_{j=1}^{j=i+1} \left( \frac{\partial I}{\partial Z_{j-1}} \cdot \delta Z_{j-1} \right)^2 + \sum_{j=1}^{j=i+1} \left( \frac{\partial I}{\partial V_{j-1}} \cdot \delta V_{j-1} \right)^2} \quad (\text{A-17})$$

For each related pair,  $Z_j$  and  $V_j$ , of a data set, the uncertainty in both members of the pair may be lumped into one of the members  $V_j$ , with the other member  $Z_j$  being considered exact. Consequently, the right-hand side of Eq. (A-17) may be simplified so that  $\delta I$  may be expressed as:

$$\delta I = \sqrt{\sum_{j=1}^{j=i+1} \left( \frac{\partial I}{\partial V_{j-1}} \cdot \delta V_{j-1} \right)^2} \quad (\text{A-18})$$

This expression implies the taking of the partial derivation of  $I$  with respect to each of the series of variables  $V_0, V_1, \dots, V_{j-1}, V_j, V_{j+1}, \dots, V_{i-1}, V_i$ . The quantity  $I$  is itself expressed as a series, formed in such a manner that each member of the series  $V_0$  to  $V_i$ , except these two end values, appears in two successive terms of the series. Thus, in semi-expanded form, the integral term of Eq. (A-16) may be expressed as:

$$\begin{aligned} I = & -g \left\{ (Z_1 - Z_0) [\ln(V_1/V_0)]^{-1} (V_1 - V_0) + (Z_2 - Z_1) [\ln(V_2/V_1)]^{-1} (V_2 - V_1) \right. \\ & + \dots + (Z_j - Z_{j-1}) [\ln(V_j/V_{j-1})]^{-1} (V_j - V_{j-1}) \\ & + (Z_{j+1} - Z_j) [\ln(V_{j+1}/V_j)]^{-1} (V_{j+1} - V_j) + \dots \\ & + (Z_{i-1} - Z_{i-2}) [\ln(V_{i-1}/V_{i-2})]^{-1} (V_{i-1} - V_{i-2}) \\ & \left. + (Z_i - Z_{i-1}) [\ln(V_i/V_{i-1})]^{-1} (V_i - V_{i-1}) \right\}. \end{aligned} \quad (\text{A-19})$$

The consequence of this expression is that the partial derivative of  $I$  with respect to  $V_0$ , and the partial derivative of  $I$  with respect to  $V_i$  both result in expressions involving only one term of the series approximation of  $I$ . The partial derivative of  $I$

with respect to all other members of the series of variables, i.e.,  $V_1$  to  $V_{i-1}$  results in expressions involving two successive terms of the series approximation of I. Thus:

$$\sqrt{\sum_{j=1}^{j=i+1} \left( \frac{\partial I}{\partial V_{j-1}} \cdot \delta V_{j-1} \right)^2} = g \sqrt{\sum_{j=1}^{j=i-1} \left[ \left( (z_j - z_{j-1}) \left( \frac{\frac{V_{j-1}}{V_j} - 1 + \left[ \ln(V_j/V_{j-1}) \right]}{\left[ \ln(V_j/V_{j-1}) \right]^2} \right) + (z_{j+1} - z_j) \left( \frac{\frac{V_{j+1}}{V_j} - 1 + \left[ \ln(V_{j+1}/V_j) \right]}{\left[ \ln(V_{j+1}/V_j) \right]^2} \right) \right) (\delta V_j) \right]^2} + \left[ (z_i - z_{i-1}) \left( \frac{\frac{V_{i-1}}{V_i} - 1 + \left[ \ln(V_i/V_{i-1}) \right]}{\left[ \ln(V_i/V_{i-1}) \right]^2} \right) (\delta V_i) \right]^2} \quad (A-20)$$

The particular arrangement of the terms under the radical sign is to emphasize the similarity of two groups of terms.

It has already been shown that, for the purposes of this study,  $\sigma\{\rho\}$  may be assumed to be a simple exponential function of altitude varying from  $2.083 \times 10^{-3} \text{ kg m}^{-3}$  at 28 kilometers to  $3.687 \times 10^{-8} \text{ kg m}^{-3}$  at 108 kilometer altitude. Since  $r\{\rho, p\}$  usually has a value between 0.6 and 1.0, and never exceeds 1.0, we may approximate  $r\{\rho, p\}$  by unity of all altitudes, in which case:

$$V = \sigma\{\rho\} \cong k e^{-\alpha z} \quad (A-21)$$

where

$$k = 9.592 \times 10^{-2}$$

$$\alpha = 1.368 \times 10^{-4}$$

If the altitude increments of successive terms on the right-hand side of Eq. (A-20) are equal, the uncertainty expression can be considerably simplified since:

$$\frac{V_1}{V_0} = \frac{V_j}{V_{j-1}} = \frac{V_{j+1}}{V_j} = \frac{V_i}{V_{i-1}} = e^{\alpha \Delta z} \equiv a = 1.1466 \quad (A-22)$$

$$\frac{V_{j-1}}{V_j} = \frac{V_{i-1}}{V_i} = \frac{1}{a} = e^{-\alpha \Delta z} \equiv b = 0.8722 \quad (\text{A-23})$$

$$\begin{aligned} \ln(V_1/V_0) &= \ln(V_j/V_{j-1}) = \ln(V_{j+1}/V_j) = \ln(V_i/V_{i-1}) \\ &= \ln a = \alpha \Delta z \equiv d = 0.1368 \end{aligned} \quad (\text{A-24})$$

With the above listed simplifications, Eq. (A-20) can be rewritten as:

$$\sqrt{\sum_{j=1}^{j=i+1} \left( \frac{\partial I}{\partial V_{j-1}} \cdot \delta V_{j-1} \right)^2} = g \sqrt{\sum_{j=1}^{j=i-1} \left\{ (z_j - z_{j-1}) \left( \frac{b - 1 + d}{d^2} \right) + (z_{j+1} - z_j) \left( \frac{a - 1 - d}{d^2} \right) \right\}^2 (\delta V_j)^2 + \left\{ (z_1 - z_0) \left( \frac{a - 1 - d}{d^2} \right) \right\}^2 (\delta V_0)^2 + \left\{ (z_i - z_{i-1}) \left( \frac{b - 1 + d}{d^2} \right) \right\}^2 (\delta V_i)^2} \quad (\text{A-25})$$

The radical on the right-hand side of this equation encompasses a series of  $(i + 1)$  terms, each of which contains an uncertainty factor  $\delta V_j$ . This factor varies from term to term in accordance with term number and in accordance with the number of the members of the corresponding set of values of  $V_j$  comprising a part of the data set. In addition to the uncertainty factor, each of these terms includes a factor representing that portion of the altitude range to which the particular uncertainty  $\delta V_j$  applies. For the first term of the series, corresponding to  $\delta V_0$ , the altitude factor consists of a single altitude element  $(z_1 - z_0)$  multiplied by a dimensionless coefficient  $[(a - 1 - d)/d^2]$  which will hereafter be called  $F$ . The altitude factor of the last term of the series corresponding to  $\delta V_i$ , also consists of a single altitude element multiplied by a different dimensionless coefficient  $[(b - 1 + d)/d^2]$  which will hereafter be called  $L$ . The remaining terms under the radical, those terms corresponding to the general uncertainty factor  $\delta V_j$ , all have altitude factors consisting of two terms. One of these terms consists of the altitude element  $(z_j - z_{j-1})$  multiplied by the dimensionless coefficient  $L$ . The other term of the altitude factor consists

of the altitude element  $(z_{j+1} - z_j)$  multiplied by the coefficient  $F$ . These two altitude elements  $(z_j - z_{j-1})$  and  $(z_{j+1} - z_j)$  are the two elements which are separated by  $z_j$ , the altitude corresponding to  $\delta V_j$ .

If  $(z_j - z_{j-1})$  is equal to  $(z_{j+1} - z_j)$ , i.e., if all the altitude elements are equal to a fixed amount  $\Delta z$ , Eq. (A-25) reduces to:

$$\delta I = g \cdot \Delta z \sqrt{(F \cdot \delta V_0)^2 + \left[ (L + F)^2 \sum_{j=1}^{j=i+1} (\delta V_j)^2 \right] + (L \cdot \delta V_i)^2} \quad (\text{A-26})$$

If the other assumptions, which lead to the series of Eqs. (A-21) to (A-24), are applied to the coefficients defined as  $F$  and  $L$ , these coefficient may be defined in terms of  $\alpha \cdot \Delta z$ :

$$F \equiv \frac{a - 1 - d}{d^2} = \frac{e^{\alpha \cdot \Delta z} - \alpha \cdot \Delta z - 1}{(\alpha \cdot \Delta z)^2} \quad (\text{A-27})$$

$$L \equiv \frac{b - 1 + d}{d^2} = \frac{e^{-\alpha \cdot \Delta z} + \alpha \cdot \Delta z - 1}{(\alpha \cdot \Delta z)^2} \quad (\text{A-28})$$

Then, for  $\Delta Z = 1000$  m,  $\alpha \cdot \Delta Z = 0.1368$ ,  $a = e^{\alpha \cdot \Delta Z} = 1.1466$ ,  $b = e^{-\alpha \cdot \Delta Z} = 0.8722$ ,  $F = 0.5236$ ,  $L = 0.4780$ , and  $F + L = 1.0016$ . If the values of the members of the set  $\delta V_0, \dots, \delta V_j, \dots, \delta V_i$  are known,  $\delta I$  the uncertainty of the integral may be calculated.

For purposes of illustration, it is assumed that each member of the set of  $\delta V_j$  is 6 percent of the corresponding member of the set  $V_j$ . Thus, consecutive members of the set  $\delta V_0, \dots, \delta V_j, \dots, \delta V_i$  form a geometric series with a common ratio "a" previously defined to be 1.1466. Eq. (A-26), however, calls for the sum of squares of the members of the set  $\delta V_j$ , i.e.,

$$\sum_{j=1}^{j=i+1} (\delta V_j)^2.$$

The members of this set  $(\delta V_j)^2$  also form a geometric series with the common ratio  $a^2$ , such that:

$$(F + L)^2 \sum_{j=1}^{j=i-1} (\delta V_j)^2 = (F + L)^2 \left[ \frac{(\delta V_{i-1})^2 \cdot a^2 - (\delta V_1)^2}{a^2 - 1} \right]$$

(A-29)

Evaluating this expression as a part of Eq. (A-26) on the basis of the specified conditions, yields a value  $2.26 \text{ nt m}^{-2}$  for  $\delta I$ , or 1.54 percent of  $1.45 \times 10^2 \text{ nt m}^{-2}$ , the 28 kilometer value of  $\sigma\{p\}$ . It is interesting to note that for a sufficiently large number of increments in the integration, the percentage uncertainty of the entire integral is considerably less than the percentage uncertainty of any single element. This situation suggests that observations of  $V_j$  be made at reasonably close altitude intervals.

It can also be shown that since the absolute uncertainty grows exponentially with decreasing altitude (for a fixed relative uncertainty), the lowest 17-km region of the integration, within which the value of  $V$  changes by a factor of 10 contributes about 99 percent of the total uncertainty in  $\delta I$ . Thus, even if the percent uncertainty in the values of  $V_j$  at the upper end of the range of integration in excess of 40 km should be found to be very large, these large percent uncertainties would contribute very little to the uncertainty in  $I$  at the lower altitudes.

#### SUMMARY

The following statements regarding computational procedures have been demonstrated either explicitly or implicitly in this appendix.

- (1) Only downward integration of  $VdZ$ , implying the sum of positive values of  $V$  and  $I$  is generally acceptable for computing  $\sigma\{p\}$  over extended ranges of altitude.
- (2) Any of a number of reasonable quadrature formulas will introduce less uncertainty in  $\sigma\{p\}$  than is introduced by the uncertainty in the observed values of  $V$ .

- (3) The greater the number of observations of  $V$  within a particular altitude range, the smaller will be the uncertainty in the computed values of  $\sigma\{p\}$ .
- (4) When the range of altitudes involved in a particular set of data of  $V$  vs  $Z$ , extends for 50 or more kilometers, the uncertainties in  $V$  at the high-altitude end of the range have little influence on the uncertainty in the computer values of  $\sigma\{p\}$  at the low-altitude end of the range of observation.

## REFERENCES

1. Minzner, R.A., and Ripley, W.S.: ARDC Model Atmosphere, 1956. Air Force Surveys in Geophysics No. 86 (AFCRC TN-56-204), 1956.
2. Minzner, R.A., Ripley, W.S., and Condrion, T.P.: U.S. Extension to the ICAO Standard Atmosphere. U.S. Govt. Printing Office, Washington, D.C., 1958.
3. Minzner, R.A., Champion, K.S., and Pond, H.L.: The ARDC Model Atmosphere, 1959. ARDC-TR-59-267, Air Force Surveys in Geophysics, No. 115 (AFCRC-TR-59-267), 1959.
4. Smith, O.E.: A Reference Atmosphere for Patrick Air Force Base, Florida (Annual). NASATND-595, 1961.
5. Court, A., Kantor, A.J., and Cole, A.E.: Supplemental Atmospheres. Research Note, AFCRL-62-899, 1962.
6. Cole, A.E., and Kantor, A.J.: Air Force Interim Supplemental Atmospheres to 90 km. Air Force Surveys in Geophysics, No. 153 (AFCRL-63-936), 1963.
7. U.S. Standard Atmosphere, 1962. National Aeronautics and Space Administration, U.S. Air Force, and U.S. Weather Bureau, Govt. Printing Office, Washington, D.C.
8. Buell, C.E.: Statistical Relations in a Perfect Gas Atmosphere. Kaman Nuclear, Colorado Springs, Colo., 1965.
9. Buell, C.E.: Some Relations Among Atmospheric Statistics. J. Meteorol., 11, 1954, pp. 238-244.
10. Stidd, C.K.: A Note on the Application of the Hydrostatic Equation to Atmospheric Statistics. J. Meteorol., 11, 1954. pp. 165-166.
11. Minzner, R.A., and Morgenstern, P.: Range and Structure of Ambient Density from 30 to 120 km Altitude. Final Report, GCA-TR-68-15-N (Contract NAS8-220098), GCA Corp., Bedford, Mass., 1968.
12. Minzner, R.A., Morgenstern, P., and Mello, S.: Tabulations of Atmospheric Density, Temperature and Pressure from 437 Rocket and Optical-Probe Soundings During the Period 1947 to early 1965. GCA-TR-67-10-N (Contracts NASw-1463 and NASw-1225), GCA Corp., Bedford, Mass., 1967.



## REFERENCES (Continued)

13. Scarborough, J.B.: Numerical Mathematical Analysis, 2nd Edition. Johns Hopkins Press, Baltimore, Md., 1950.
14. Wood, C.P., and Spreen, W.C.: An Investigation of the Relation Among Some Statistics for Upper-air Pressure, Temperature, and Density. J. Appl. Meteorol., 2, 1963, pp. 292-297.
15. Minzner, R.A.: Second Quarterly Report, (Contract NASw-1225), GCA Corp., Bedford, Mass., 1965.
16. List, R.S., ed.: Smithsonian Meteorological Tables, 6th edition. Publication 4014, Smithsonian Misc. Collec., vol. 114, 1951.
17. Minzner, R.A., and Mello, S.: Geopotential versus Geometric Altitude from 0 to 10,000 Kilometers for Various Latitudes. Scientific Report, GCA-TR-66-20N (Contract NASw-1463), GCA Corp., Bedford, Mass., 1967.
18. Minzner, R.A., Sauermann, G.O., and Faucher, G.A.: Low Mesopause Temperatures over Eglin Test Range Deduced from Density Data. J. Geophys. Res., 70, 1965, pp. 739-742.
19. Minzner, R.A., and Sauermann, G.O.: Temperature Determination of Planetary Atmospheres - Optimum Boundary Conditions for both Low and High Solar Activity. Scientific Report, GCA-TR-66-6N (Contract NASw-1225), GCA Corp., Bedford, Mass., 1966.

NATIONAL AERONAUTICS AND SPACE ADMINISTRATION

WASHINGTON, D. C. 20546

OFFICIAL BUSINESS

PENALTY FOR PRIVATE USE \$300

FIRST CLASS MAIL



POSTAGE AND FEES PAID  
NATIONAL AERONAUTICS AND  
SPACE ADMINISTRATION

07U 001 38 51 3DS 71088 00903  
AIR FORCE WEAPONS LABORATORY /WL0L/  
KIRTLAND AFB, NEW MEXICO 87117

ATT E. LOU BOWMAN, CHIEF, TECH. LIBRARY

POSTMASTER: If Undeliverable (Section 158  
Postal Manual) Do Not Return

*"The aeronautical and space activities of the United States shall be conducted so as to contribute . . . to the expansion of human knowledge of phenomena in the atmosphere and space. The Administration shall provide for the widest practicable and appropriate dissemination of information concerning its activities and the results thereof."*

— NATIONAL AERONAUTICS AND SPACE ACT OF 1958

## NASA SCIENTIFIC AND TECHNICAL PUBLICATIONS

**TECHNICAL REPORTS:** Scientific and technical information considered important, complete, and a lasting contribution to existing knowledge.

**TECHNICAL NOTES:** Information less broad in scope but nevertheless of importance as a contribution to existing knowledge.

**TECHNICAL MEMORANDUMS:** Information receiving limited distribution because of preliminary data, security classification, or other reasons.

**CONTRACTOR REPORTS:** Scientific and technical information generated under a NASA contract or grant and considered an important contribution to existing knowledge.

**TECHNICAL TRANSLATIONS:** Information published in a foreign language considered to merit NASA distribution in English.

**SPECIAL PUBLICATIONS:** Information derived from or of value to NASA activities. Publications include conference proceedings, monographs, data compilations, handbooks, sourcebooks, and special bibliographies.

**TECHNOLOGY UTILIZATION PUBLICATIONS:** Information on technology used by NASA that may be of particular interest in commercial and other non-aerospace applications. Publications include Tech Briefs, Technology Utilization Reports and Technology Surveys.

*Details on the availability of these publications may be obtained from:*

**SCIENTIFIC AND TECHNICAL INFORMATION OFFICE**

**NATIONAL AERONAUTICS AND SPACE ADMINISTRATION**

**Washington, D.C. 20546**